Click here to view PowerPoint presentation; Press Esc to exit

Mitigation of Ionospheric Effects on High Frequency Surface Wave Radar

Dr. Ryan J. Riddolls
Defence R&D Canada - Ottawa
3701 Carling Avenue
Ottawa, Ontario K1A 0Z4
Canada
ryan.riddolls@drdc-rddc.gc.ca

ABSTRACT

High Frequency Surface Wave Radar (HFSWR) takes advantage of the diffraction of electromagnetic waves over the conducting ocean surface to detect, locate, and track surface vessels beyond the line-of-sight horizon of the earth. However, long-range surface vessel detection is often confounded by radar clutter comprising echoes from the ionospheric plasma. In this paper, we characterize the angular spectrum of these reflections, and from this information deduce the signal-to-clutter processing gain that can be realized by various adaptive receive antenna array configurations. In particular, it is shown that there is advantage to be realized by sampling ionospheric echoes with a planar two-dimensional array rather than a conventional linear one-dimensional HFSWR array. Using a planar array, the radar can distinguish high-elevation ionospheric clutter signals from low-elevation surface target echoes.

1 ADAPTIVE ARRAYS

Ionospheric reflection in HFSWR applications complicates the detection of weak target echoes. In particular, during nighttime Spread F conditions, ionospheric clutter can occupy most of the far ranges in the radar range-Doppler search plane. Adaptive antenna array techniques can be used to increase the ratio of surface vessel echo power to ionospheric clutter power in cluttered radar ranges.

We consider a surface vessel radar echo consisting of a plane wave of amplitude x that is received by an array of antenna elements arranged in an arbitrary configuration. The amplitude and phase response of the individual sensors to the plane wave is captured by an array manifold vector $\mathbf{v}$. In addition to the plane wave signal, the sensors are corrupted by a "noise" vector $\mathbf{n}$ that is dominated by ionospheric clutter signals. Thus the signal measured by the array can be written as $\mathbf{y} = \mathbf{v}x + \mathbf{n}$.

We assume the radar signals are narrowband such that they can be described by complex amplitudes. We devise a linear estimator for x that consists of summing the measured signals according to a "weight" function $\mathbf{w}$. This estimator is denoted as $\hat{x} = \mathbf{w}^H\mathbf{y}$, where H is the complex conjugate transpose. In order to minimize the variance of the expected value $E(\hat{x})$ under the constraint of no distortion $E(\hat{x}) = E(x)$, the optimal choice of weights in this linear estimator is given by [1]:

$$\mathbf{w}^H = \frac{\mathbf{v}^H\mathbf{R}_n^{-1}}{\mathbf{v}^H\mathbf{R}_n^{-1}\mathbf{v}}, \tag{1}$$

where $\mathbf{R}_n = E(\mathbf{n}\mathbf{n}^H)$ is the noise covariance matrix. This estimator is an adaptive beamformer, providing constructive interference in the target direction and destructive interference in noise directions.

Riddolls, R.J. (2006) Mitigation of Ionospheric Effects on High Frequency Surface Wave Radar. In *Characterising the Ionosphere* (pp. 20-1 – 20-6). Meeting Proceedings RTO-MP-IST-056, Paper 20. Neuilly-sur-Seine, France: RTO. Available from: http://www.rto.nato.int/abstracts.asp.

Report Documentation Page

Form Approved
OMB No. 0704-0188

1. REPORT DATE	2. REPORT TYPE	3. DATES COVERED
01 JUN 2006	**N/A**	**-**

4. TITLE AND SUBTITLE	5a. CONTRACT NUMBER
Mitigation of Ionospheric Effects on High Frequency Surface Wave Radar	5b. GRANT NUMBER
	5c. PROGRAM ELEMENT NUMBER
6. AUTHOR(S)	5d. PROJECT NUMBER
	5e. TASK NUMBER
	5f. WORK UNIT NUMBER
7. PERFORMING ORGANIZATION NAME(S) AND ADDRESS(ES) **Defence R&D Canada - Ottawa 3701 Carling Avenue Ottawa, Ontario K1A 0Z4 Canada**	8. PERFORMING ORGANIZATION REPORT NUMBER
9. SPONSORING/MONITORING AGENCY NAME(S) AND ADDRESS(ES)	10. SPONSOR/MONITOR'S ACRONYM(S)
	11. SPONSOR/MONITOR'S REPORT NUMBER(S)

12. DISTRIBUTION/AVAILABILITY STATEMENT
Approved for public release, distribution unlimited

13. SUPPLEMENTARY NOTES
See also ADM002065., The original document contains color images.

14. ABSTRACT

15. SUBJECT TERMS

16. SECURITY CLASSIFICATION OF:			17. LIMITATION OF ABSTRACT	18. NUMBER OF PAGES	19a. NAME OF RESPONSIBLE PERSON
a. REPORT	b. ABSTRACT	c. THIS PAGE			
unclassified	**unclassified**	**unclassified**	**UU**	**38**	

This beamformer is distortionless, so it provides no improvement in target signal power. All SNR improvement arises from reducing noise power associated with the ionospheric clutter. At the input to the beamformer, the noise power received by individual antenna elements is given by the diagonal entries of $\mathbf{R}_n$. To help quantify the reduction in this noise power by the beamformer, we assume the noise power is the same at all sensors, and equal to a scalar denoted by R_n. The noise power at the output of the beamformer is given by

$$R_{\hat{x}} = \mathbf{w}^H \mathbf{R}_n \mathbf{w} = \frac{1}{\mathbf{v}^H \mathbf{R}_n^{-1} \mathbf{v}}. \tag{2}$$

Therefore, the SNR gain due to the array, denoted as the "array gain", is given by

$$A = R_n / R_{\hat{x}} = R_n \mathbf{v}^H \mathbf{R}_n^{-1} \mathbf{v} \equiv \mathbf{v}^H \boldsymbol{\rho}_n^{-1} \mathbf{v}. \tag{3}$$

Here, $\boldsymbol{\rho}_n$ is a normalized covariance matrix where the entries on the matrix diagonal are unity. In the case of uncorrelated noise, the array gain will be simply $A = \mathbf{v}^H \mathbf{v} = N$, where N is the number of sensors. In the case of correlated noise, the array gain could be more or less than N.

2 DIRECTIONAL SPECTRUM OF IONOSPHERIC ECHOES

To estimate $\boldsymbol{\rho}_n$ for arbitrary receive arrays, we can characterize the ionospheric echo as a spectrum of plane waves $S(\mathbf{k}, \omega)$ incident on the array, where $\mathbf{k}$ is a vector wavenumber (k_x, k_y, k_z), and ω is the wave frequency. In the case of free space, $S(\mathbf{k}, \omega)$ reduces to a two-dimensional distribution of horizontal wavenumbers $S(k_x, k_y)$ since ω is fixed at the radar carrier frequency and the vertical wavenumber k_z is equal to $k_z = \sqrt{(\omega/c)^2 - k_x^2 - k_y^2}$ by the freespace dispersion relation $\omega = c|\mathbf{k}|$. $S(k_x, k_y)$ is equivalent to the distribution of wave direction of arrival (DOA) in elevation and azimuth.

To estimate $S(k_x, k_y)$ we extend to two dimensions a method that was devised for the characterization of one-dimensional plasma turbulence using fixed probe pairs [2]. The plane wave spectrum $S(k_x, k_y)$ is related to the plane wave spatial autocorrelation function R by

$$\frac{1}{(2\pi)^2} \iint dk_x \, dk_y \, S(k_x, k_y) e^{ik_x X + ik_y Y} = R(X, Y), \tag{4}$$

where X and Y are the lags in the x and y directions, and the autocorrelation function R is defined as

$$R(X, Y) = E[\Phi^*(x, y) \Phi(x + X, y + Y)]. \tag{5}$$

Here, Φ is a wave field with random amplitude a and random phase θ:

$$\Phi(x, y) \quad = \quad a(x, y) e^{i\theta(x,y)}. \tag{6}$$

In analogy to instantaneous frequency in the time domain, we define local wavenumbers $K_x(x, y)$ and $K_y(x, y)$ in the spatial domain:

$$K_x(x, y) = \frac{\partial \theta(x, y)}{\partial x} \qquad K_y(x, y) = \frac{\partial \theta(x, y)}{\partial y}. \tag{7}$$

By the moment-generating property of the Fourier transform, we have that

$$\frac{1}{(2\pi)^2} \iint dk_x \, dk_y (ik_x)^M (ik_y)^N S(k_x, k_y) = \frac{\partial^M \partial^N}{\partial X^M \partial Y^N} R(X, Y) \Big|_{X,Y=0} \tag{8}$$

$$= E\left[a(x,y) e^{-i\theta(x,y)} \sum_{m=0}^{M} \sum_{n=0}^{N} \binom{M}{m} \binom{N}{n} \frac{\partial^m \partial^n}{\partial X^m \partial Y^n} a(x+X, y+Y) \frac{\partial^{M-m} \partial^{N-n}}{\partial X^{M-m} \partial Y^{N-n}} e^{i\theta(x+X,y+Y)} \right]_{X,Y=0}. \quad (9)$$

If the amplitude and wavenumber spatial variation is slow compared to a wavelength such that

$$\left| \frac{1}{a(x,y)} \frac{\partial^m a(x,y)}{\partial X^m} \right|, \left| \frac{1}{K_x(x,y)} \frac{\partial^m K_x(x,y)}{\partial X^m} \right| \ll |K_x^m(x,y)| \quad (10)$$

$$\left| \frac{1}{a(x,y)} \frac{\partial^n a(x,y)}{\partial Y^n} \right|, \left| \frac{1}{K_y(x,y)} \frac{\partial^n K_y(x,y)}{\partial Y^n} \right| \ll \left| K_y^n(x,y) \right|, \quad (11)$$

for all $m, n > 0$, then it can be shown that Equations (8) and (9) reduce to

$$\frac{1}{(2\pi)^2} \iint dk_x \, dk_y \, k_x^M k_y^N S(k_x, k_y) \approx E[a^2(x,y) K_x^M(x,y) K_y^N(x,y)]. \quad (12)$$

Since a, K_x, and K_y are random variables, they have a joint probability density function (PDF) $f(a^2, K_x, K_y)$:

$$\frac{1}{(2\pi)^2} \iint dk_x \, dk_y k_x^M k_y^N S(k_x, k_y) \approx \iiint da^2 \, dK_x \, dK_y \, a^2(x,y) K_x^M(x,y) K_y^N(x,y) f(a^2, K_x, K_y), \quad (13)$$

and so the plane wave spectrum in the vicinity of the receive array can be written

$$S(k_x, k_y) \approx (2\pi)^2 \int da^2 \, a^2(x,y) f(a^2, K_x, K_y). \quad (14)$$

Thus the wave spectrum is proportional to a power-weighted joint PDF of the local wavenumbers. This result is analogous to the time domain result that the frequency spectrum is equal to the spectrum of instantaneous frequencies when the signal modulation rate is slow compared to the signal bandwidth.

3 DIRECTIONAL SPECTRUM MEASUREMENTS

In practice, the right side of Equation (14) can be estimated by compiling a power-weighted histogram of the phase lags from antenna pairs spaced in the x and y directions. To this end, experiments were carried out on 15 Oct 2003 at an HFSWR installation at Cape Race, Newfoundland, Canada. This facility is described in general terms in [3]. For the characterization of the ionospheric signals, the facility was operated in a ship surveillance mode at 3.2 MHz, and ionospheric Spread F clutter signals were collected by monopole receive antenna pairs that were spaced 54.0 m in the x direction (approximately southeast) and 33.3 m in the y direction (approximately northeast). The data were analyzed for phase lags and power content and the results are plotted in Figure 1.

The left panel of Figure 1 shows a set of DOA measurements where zenith is the origin of the plot and the horizon is the edge of the circle. Here, K_x is the horizontal axis, and K_y is the vertical axis. This scatter plot suggests that $S(k_x, k_y)$ depends on the radial distance $\sqrt{k_x^2 + k_y^2}$ rather than k_x and k_y individually. The center and right panels are plots of the marginal distributions $S(k_x) = \int dk_y \, S(k_x, k_y)$ and $S(k_y) = \int dk_x \, S(k_x, k_y)$, which take the form of Gaussian distributions of comparable variance. These experimental results suggest that we model the power spectrum $S(k_x, k_y)$ as an uncorrelated bivariate Gaussian distribution centered at approximately zenith:

$$S(k_x, k_y) \approx \frac{2\pi}{\sigma^2} e^{-\frac{k_x^2 + k_y^2}{2\sigma^2}}. \quad (15)$$

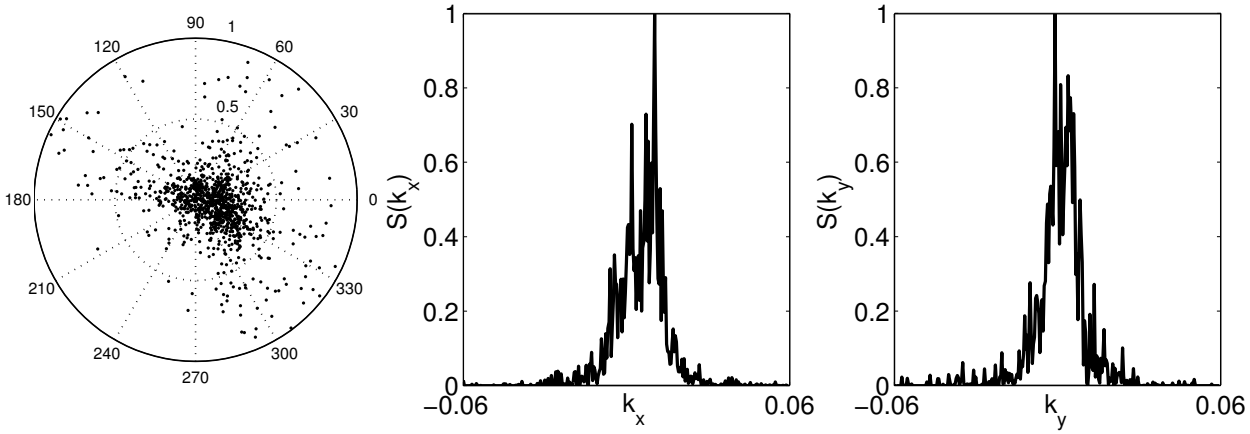

Figure 1: Left, measured DOA scatter plot. Center, measured $S(k_x)$. Right, measured $S(k_y)$.

We will retain the standard deviation σ of this distribution as a parameter in our analysis. The parameter σ is a function of the roughness of the reflecting ionospheric plasma, and describes the angular spread α of the ionospheric reflections:

$$\alpha = 2\sin^{-1}(\sigma/k). \tag{16}$$

The plots of Figure 1 suggest an angular spread α of about 16 degrees.

To compute the normalized array covariance matrix $\boldsymbol{\rho}_n$, we evaluate the spatial autocorrelation function R associated with the plane wave spectrum $S(k_x, k_y)$ at points corresponding to element locations in the receive array. The spatial autocorrelation function is given by

$$R(X,Y) = \frac{1}{(2\pi)^2}\int dk_x\, dk_y\, S(k_x,k_y)e^{ik_xX+ik_yY} = e^{-\frac{X^2+Y^2}{2/\sigma^2}}. \tag{17}$$

Thus any pair of array elements in a two-dimensional array have a correlation that decays as a Gaussian with respect to their separation in the x and y directions, where the correlation distance is $1/\sigma$. In this experiment the correlation distance is about 100 m.

4 ADAPTIVE ARRAY GAIN CALCULATIONS

We can now determine the array covariance matrix $\boldsymbol{\rho}_n$ for various array configurations by evaluating the spatial autocorrelation function R at the locations of the array elements. The adaptive array gain A for these array configurations can then be calculated according to Equation (3). This procedure has been carried out for four common array configurations, each of $N = 16$ elements and interelement spacing of $\lambda/2$. These configurations consist of (1) a 16-element linear array, (2) a cross of two 8-element linear arrays, (3) a 16-element circular array, and (4) a filled-aperture 4x4 square array. The variation in A has been calculated as a function of the azimuthal angle of the target signal with respect to array broadside, and as a function of the angular spread α of the ionosphere signals, as given by Equation (16). The results are plotted in Figure 2.

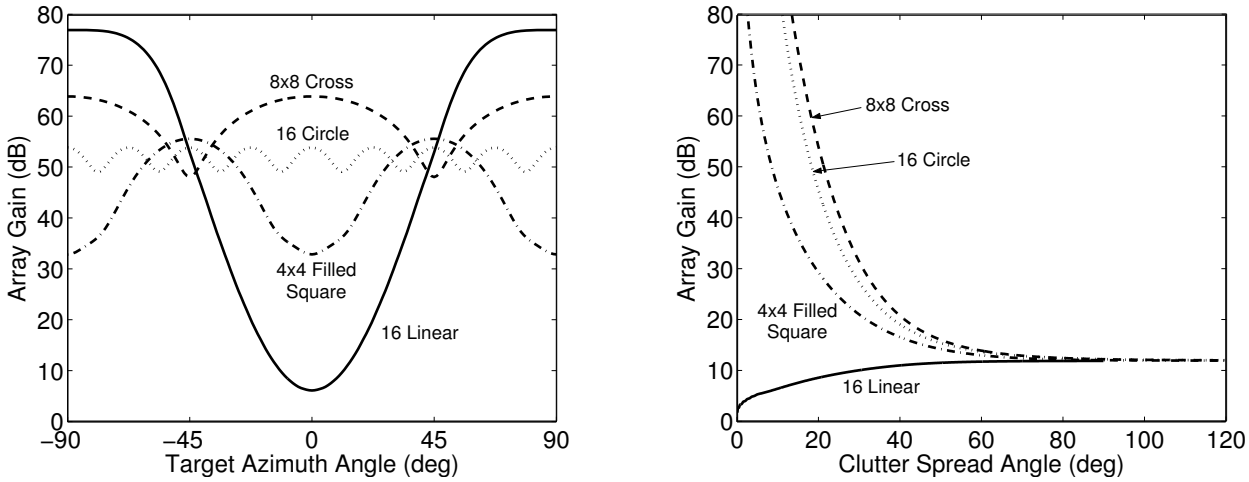

Figure 2: Left, adaptive array gain versus target azimuth angle with respect to broadside (clutter spread angle = 16 degrees). Right, adaptive array gain for broadside target versus clutter spread angle.

The results have physical interpretations as follows. The adaptive array gain for a fixed clutter spread angle (left panel of Figure 2) varies with the aperture of a projection of the array on a vertical plane oriented in the target direction. For example, when the target is broadside to the 16-element linear array, the ionospheric clutter is also broadside with respect to the array, and the array has difficulty distinguishing the low-elevation surface vessel echo from the high-elevation ionospheric echo. This effect becomes more pronounced as the clutter spread angle α goes to zero, as shown in the right panel of Figure 2. In contrast, the two-dimensional arrays have better array gains for targets near broadside due to their finite aperture projection on the vertical plane containing the target direction. The zenith array null becomes perfect when $\alpha = 0$ and the array gains for these configurations become infinite. Conversely, as α gets large, the clutter signal becomes uncorrelated noise for all array configurations, and the array gains approach the uncorrelated case of $A = N = 12$ dB.

5 REFERENCES

[1] Capon, J. (1969). High-resolution frequency-wavenumber spectrum analysis. *Proceedings of the IEEE*, *57*(8), 1408-1418.

[2] Beall, J. M., Kim, Y. C., and Powers E. J. (1982). Estimation of wavenumber and frequency spectra using fixed probe pairs. *Journal of Applied Physics*, *53*(6), 3933-3940.

[3] Ponsford, A. M., Sevgi, L., and Chan, H. C. (2001). An integrated maritime surveillance system based on high-frequency surface-wave radars, Part 2 - Operational status and system performance. *IEEE Antennas and Propagation Magazine*, *43*(5), 52-63.

DEFENCE R&D DÉFENSE

Mitigation of Ionospheric Effects on High Frequency Surface Wave Radar

Dr. Ryan J. Riddolls

15 June 2006

Defence R&D Canada
R et D pour la défense Canada

Canada

Surface Wave Propagation

- Problem: diffraction of vertical polarized waves over lossy sphere [Fock, JPM 1945, p256]

- Solve wave equation in presence of lossy boundary

Line of Sight and Surface Wave Propagation

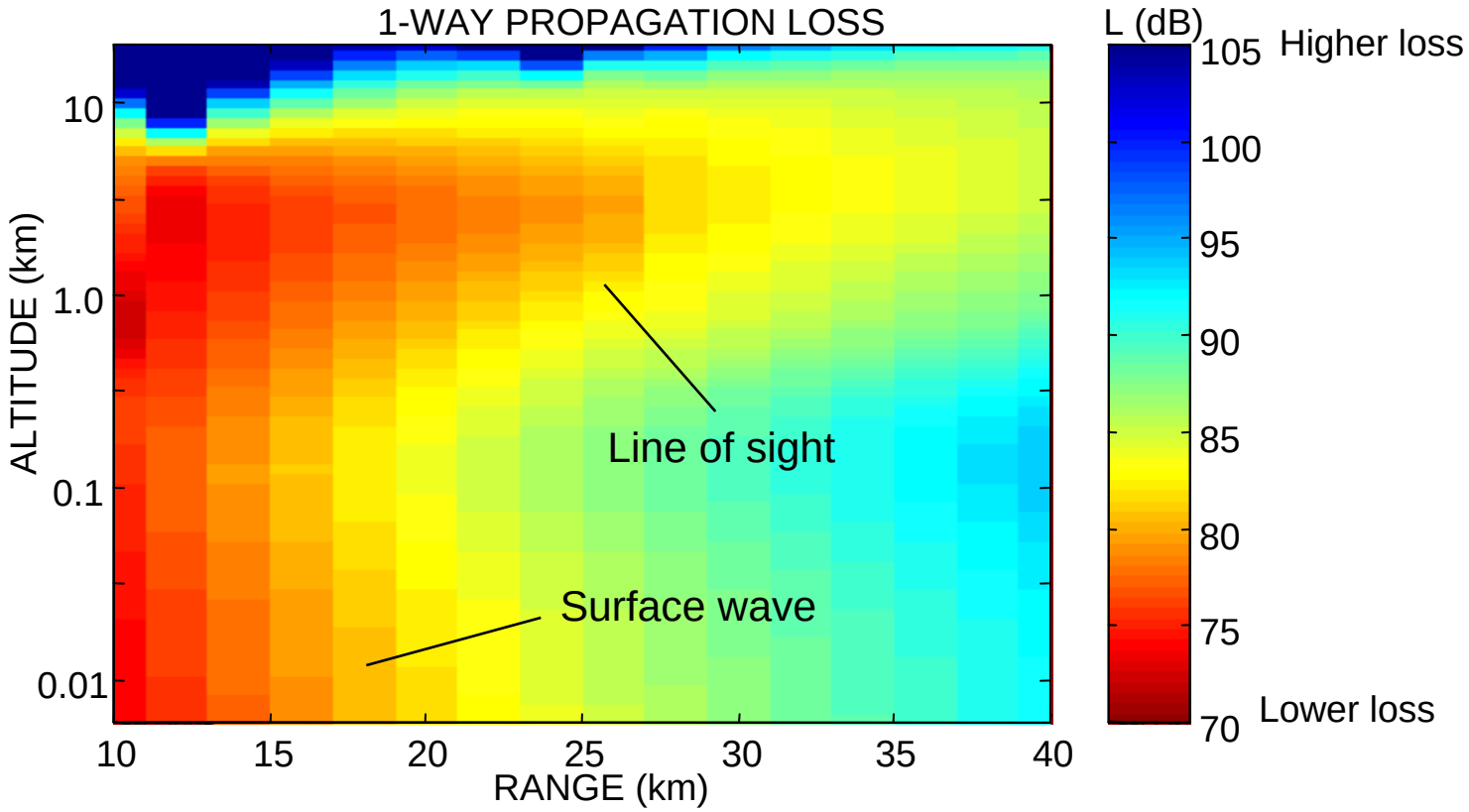

Picture courtesy Robert J. Dinger

Attenuation Curves

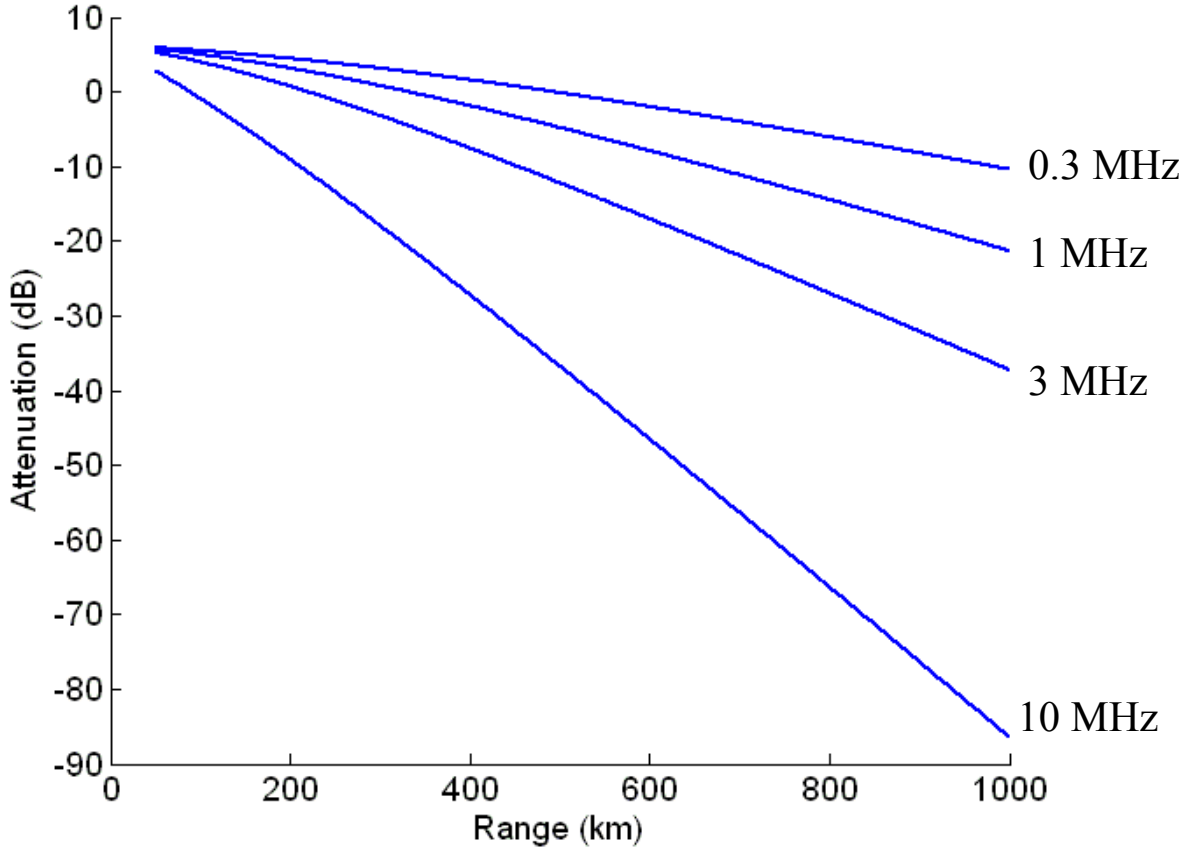

Surface Wave Radar Concept

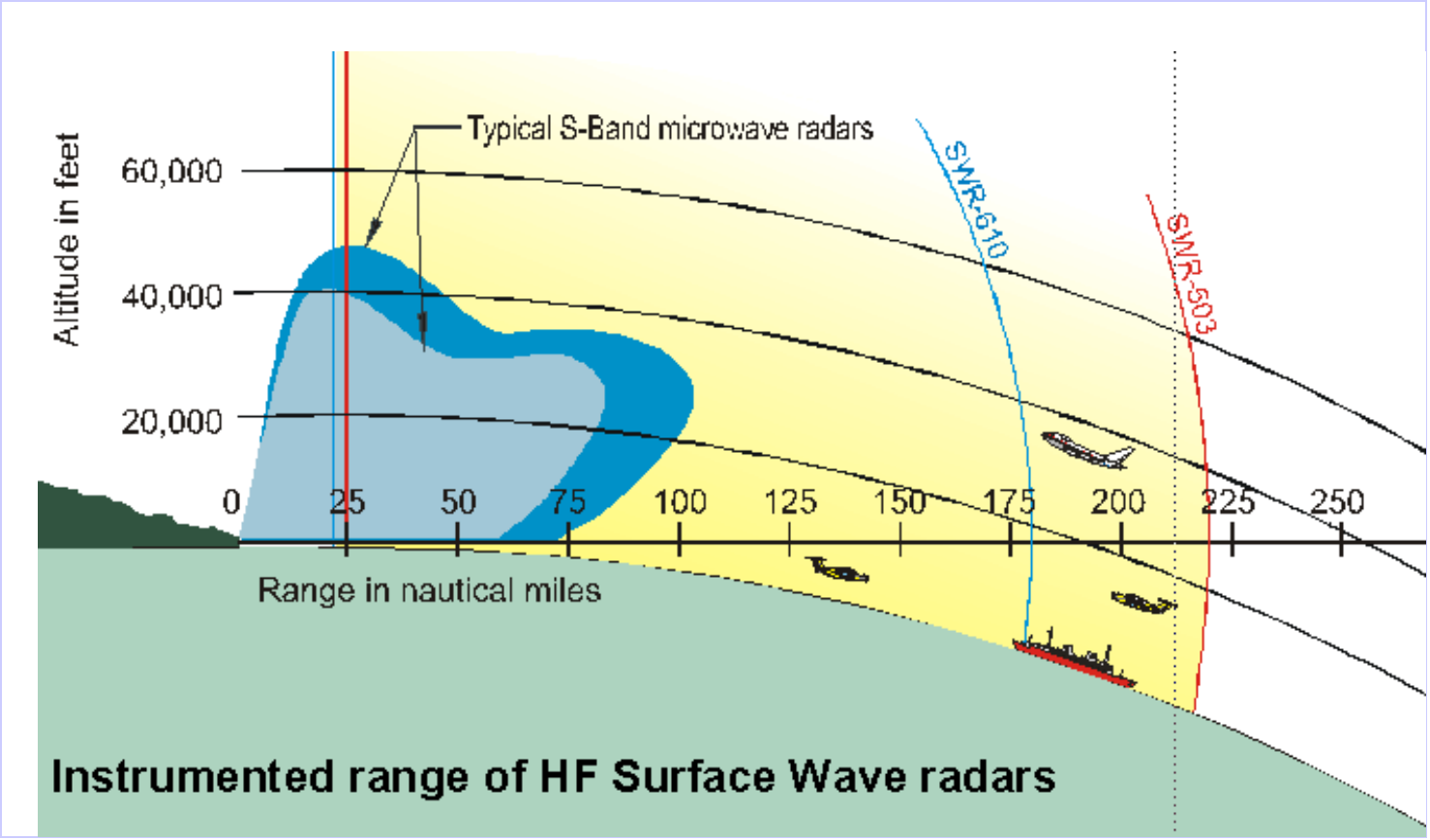

Canadian East Coast Radars

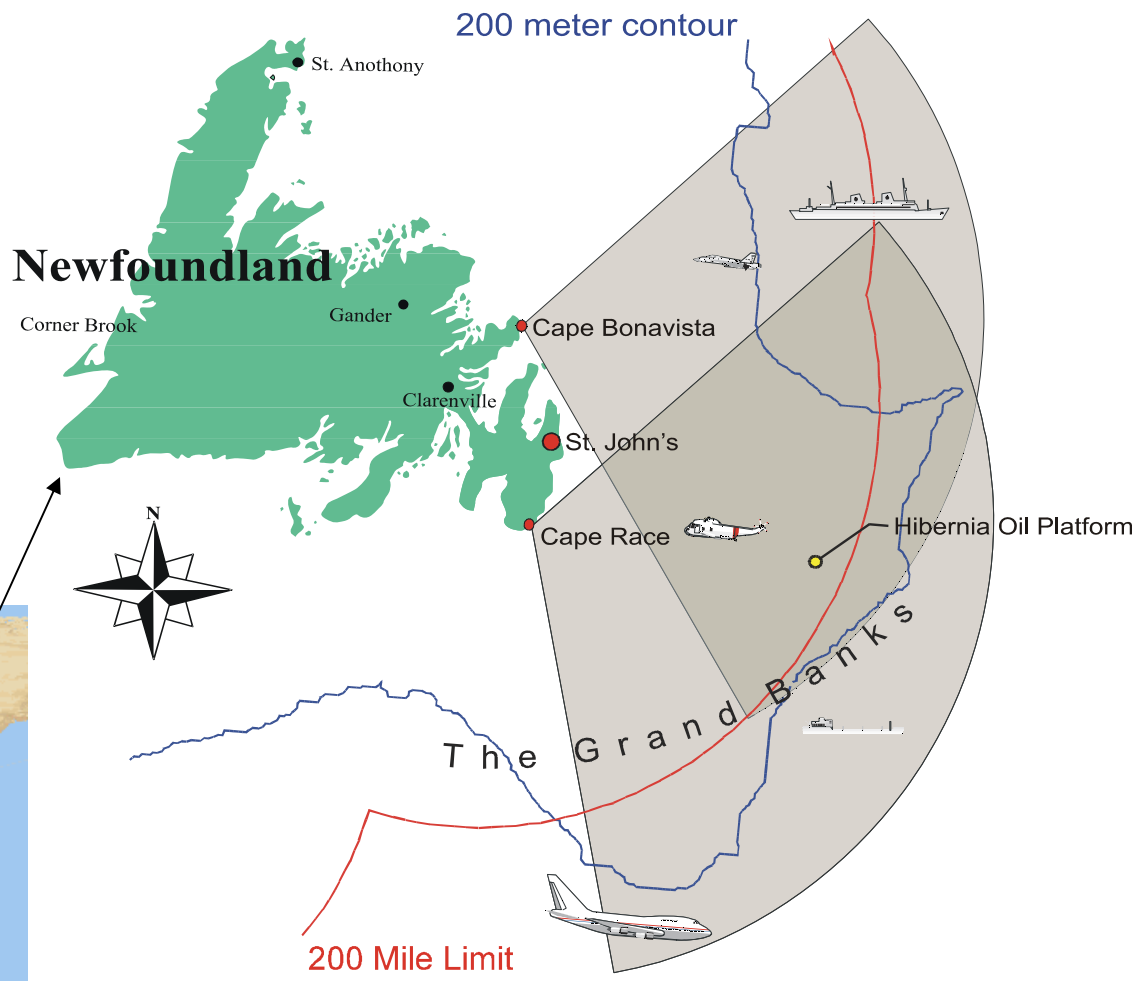

Cape Race Radar

Transmit

Receive

Cape Bonavista Radar

Transmit

Receive

Radar Configuration

• Frequency	3 - 5 MHz
• Transmit Antenna	Vertical Log Periodic
• Receive Antenna	Monopole Array
• Transmit Power	~16 kW Pulsed, 10% Duty Cycle
• PRF	up to 250 Hz
• Bandwidth	~20 kHz
• Waveform	Polyphase Codes
• Frequency Diversity	Dual Carrier Frequency
• Dwell Times	Simultaneous ~30 s, ~300 s
• Configuration	Monostatic, Bistatic, or Multistatic
• Area Coverage	+/-60 Degrees to 250 Nautical Miles

Range-Doppler: Benign Conditions

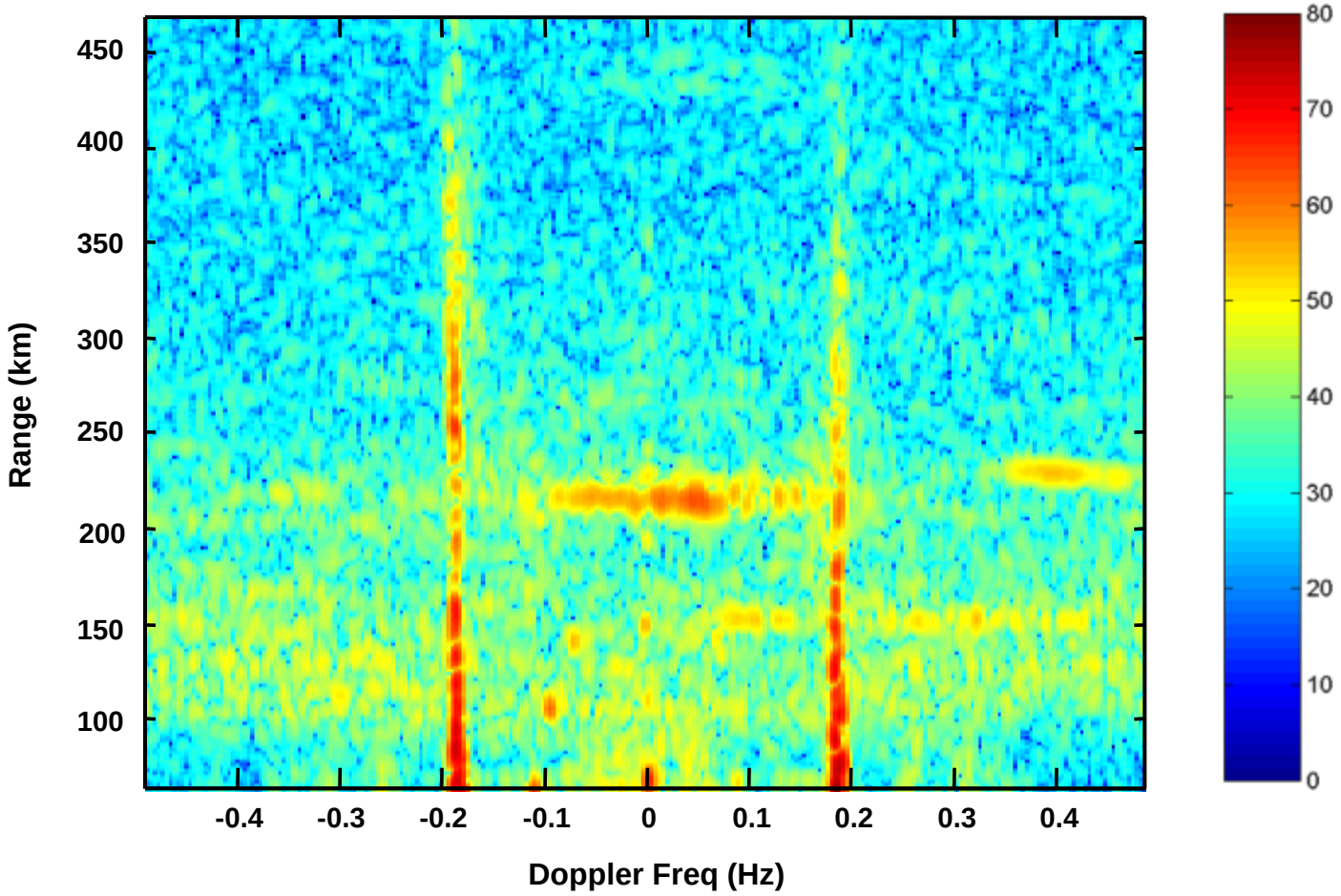

Range-Doppler: Spread F Conditions

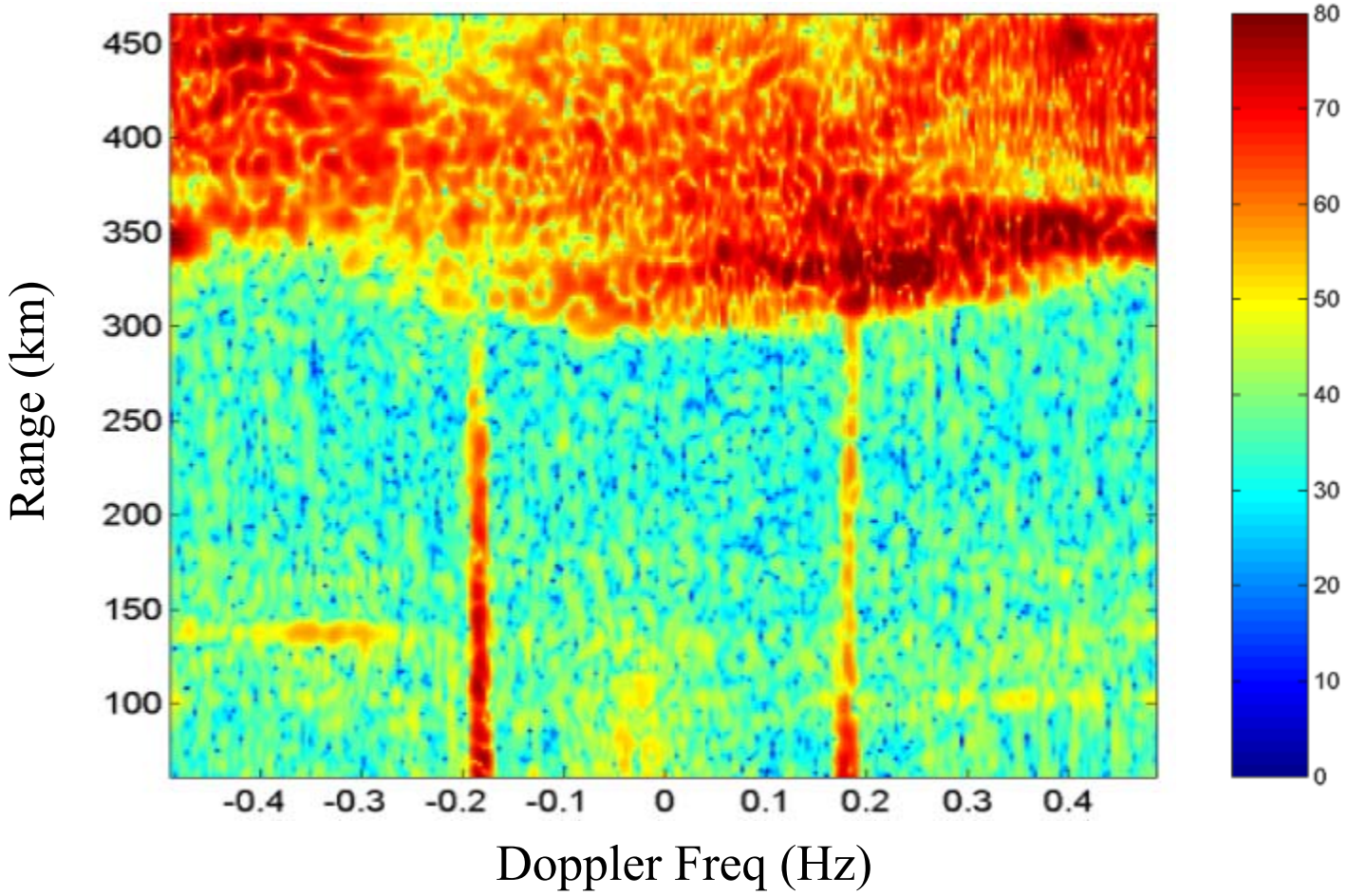

Time-Range: Evolution of Ionosphere

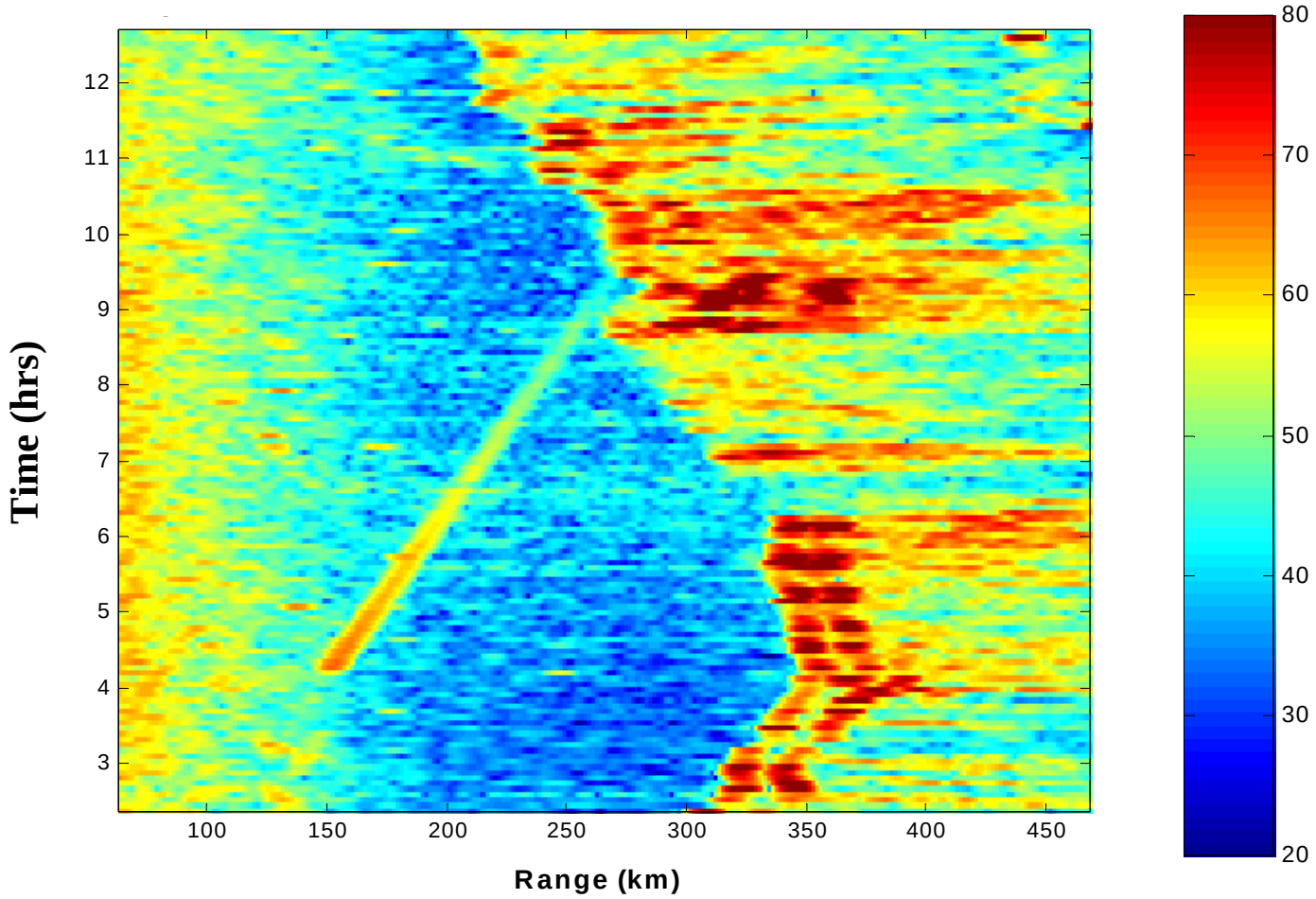

Spatial Processing: Beamforming

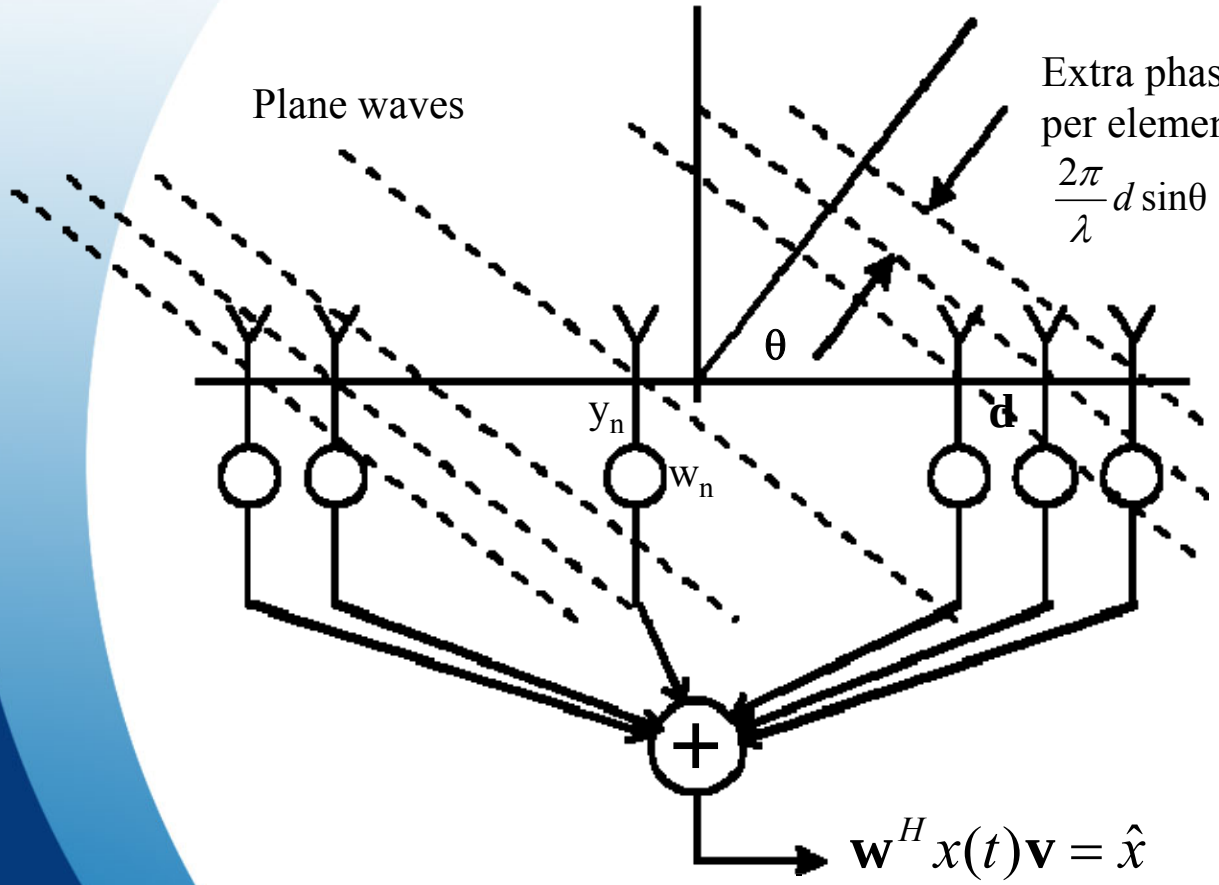

Antenna signal

$$y_n = x(t)\mathrm{e}^{in\frac{2\pi}{\lambda}d\sin\theta}$$

$$\mathbf{y} = x(t)\mathbf{v}$$

$$\mathbf{v} = [1 \;\; \mathrm{e}^{\mathrm{i}\frac{2\pi}{\lambda}d\sin\theta} \;\; \mathrm{e}^{2\mathrm{i}\frac{2\pi}{\lambda}d\sin\theta} \;\; \cdots \;\; \mathrm{e}^{(N-1)\mathrm{i}\frac{2\pi}{\lambda}d\sin\theta}]^T$$

Adaptive Beamforming

- Measured signal

$$\mathbf{y} = x\mathbf{v} + \mathbf{n}$$

- Estimate

$$\hat{x} = \mathbf{w}^H \mathbf{y}$$

- Estimation error

$$e = \mathrm{E}[(x - \hat{x})^2]$$

- Goal: minimize e under constraint

$$\mathrm{E}(\hat{x}) = x$$

Adaptive Beamforming (con'd)

- Solution

$$\mathbf{w}^H = \frac{\mathbf{v}^H \mathbf{R}_n^{-1}}{\mathbf{v}^H \mathbf{R}_n^{-1} \mathbf{v}}$$

- Noise covariance

$$\mathbf{R}_n = \mathrm{E}[\mathbf{n}\mathbf{n}^H]$$

- Output noise power

$$R_{\hat{x}} = \mathbf{w}^H \mathbf{R}_n \mathbf{w} = \frac{1}{\mathbf{v}^H \mathbf{R}_n^{-1} \mathbf{v}}$$

- If input noise is unity, then SNR gain of array is

$$A = 1 / R_{\hat{x}} = \mathbf{v}^H \mathbf{R}_n^{-1} \mathbf{v}$$

Adaptive Beamforming (con'd)

To determine A for various array configurations, we must

- Determine angular spectrum of clutter signals
- Calculate sensor covariance $\mathbf{R}_n$ for an array configuration
- Determine array gain for A for given target location

Slightly Rough Reflecting Surface

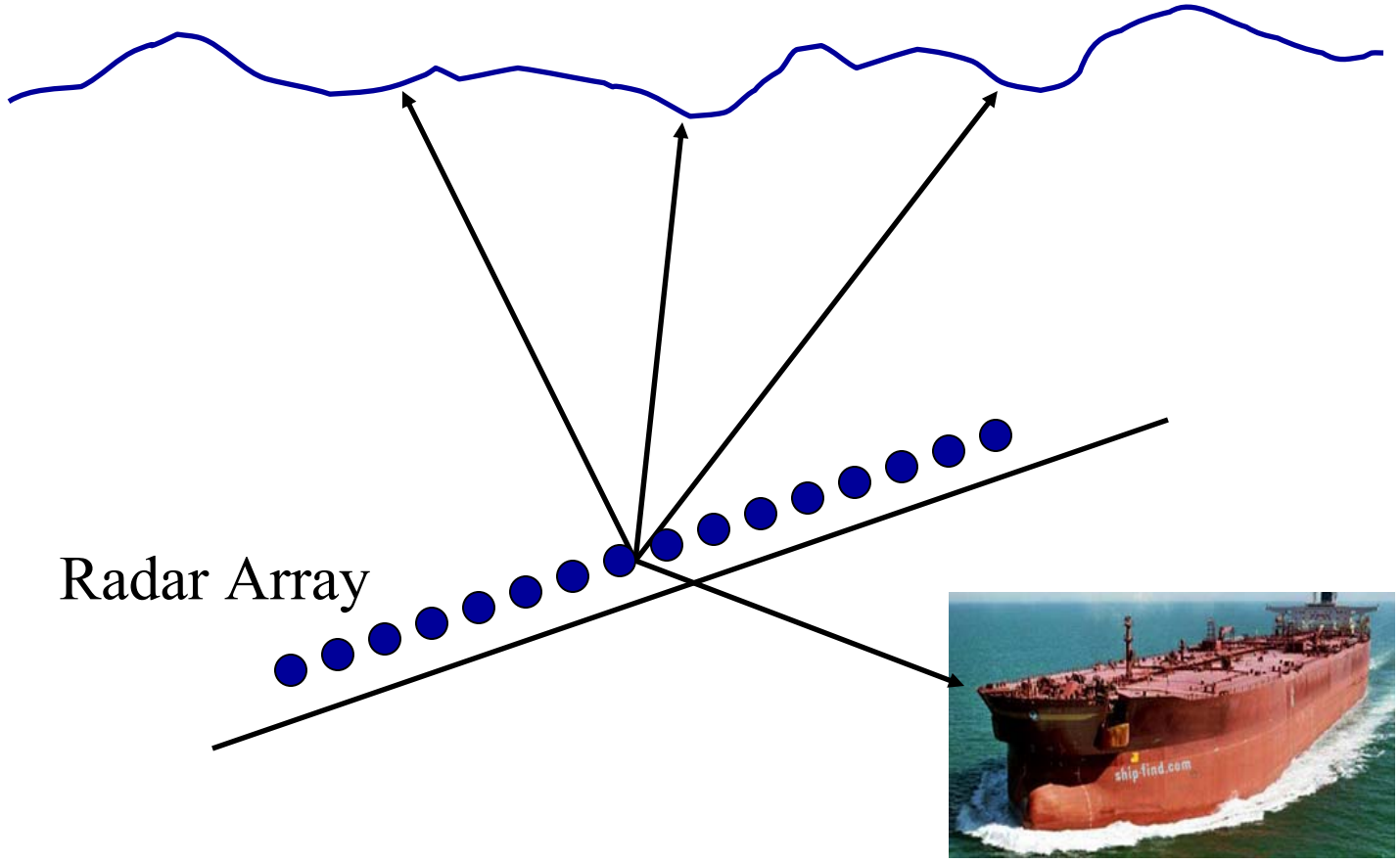

- Backscatter occurs when surface normal to incident **k**
- PDF of slopes provides PDF of reflection angles?

Slightly Rough Reflecting Surface (con'd)

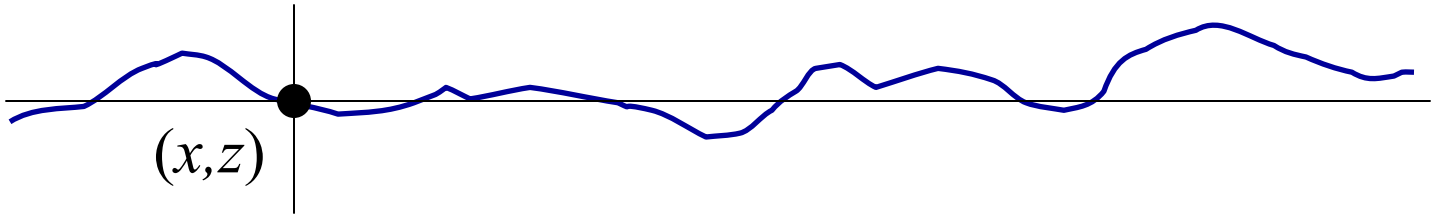

• By central limit theorem, PDF for altitude of reflecting layer at point x_1 is Gaussian:

$$f(z) = \frac{1}{\sqrt{2\pi}\sigma_z} e^{-\frac{z^2}{2\sigma_z^2}}$$

• PDF for slope z' can be derived:

$$f(z') = \frac{1}{(2\pi)^{3/2}\sigma_z\sigma_k} e^{-\frac{z'^2}{8\pi^2\sigma_z^2\sigma_k^2}}$$

where σ_k^2 is second moment of wavenumber PSD

• Typically, $\sigma_{z'} = 2\pi\sigma_z\sigma_k >> 1$, so not slightly rough!

Turbulent Plasma

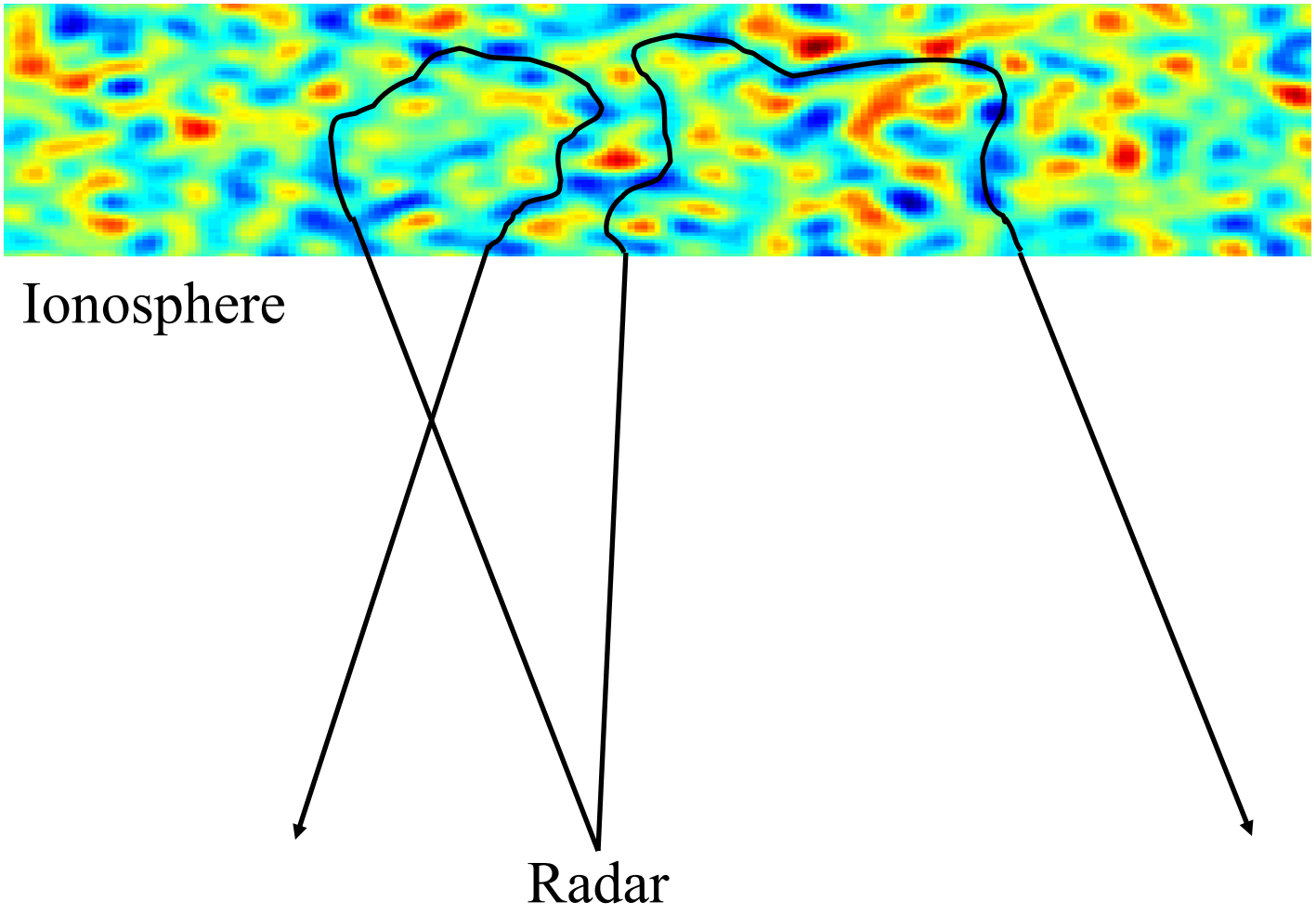

• Ray tracing can be used to determine PDF of "reflection" angles

Turbulent Plasma (con'd)

- Populate ionospheric profile with irregularities
- Choose an irregularity PSD [Hysell, JGR 1994, p15078]

$$\Delta n(k_\perp, k_\parallel) = \frac{4\pi}{\alpha k^2} \frac{2L_0 \Delta n_{rms}}{1 + k^2 L_0^2 (1 + k^2 L_1^2)}$$

$$k^2 \equiv k_\perp^2 + \frac{1}{\alpha} k_\parallel^2$$

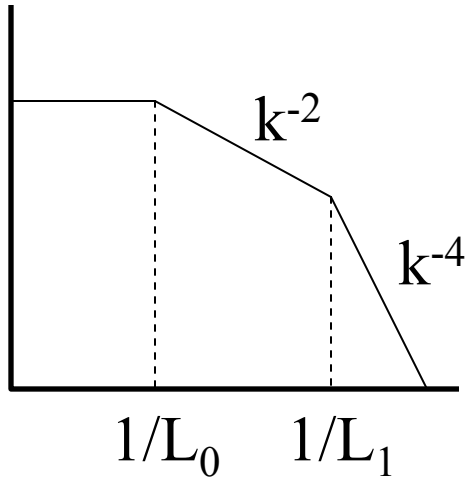

- Do ray tracing, find angular PSD of reflected signals
- Ray perturbation theory [Witte, GJI 1996, p165] shows

$$\sigma_\theta = (\Delta n_{rms} / n)\sqrt{L_{path}\sigma_k} \approx 10^{-1}$$

Ray Tracing Example

Ray Tracing Near Reflection Height

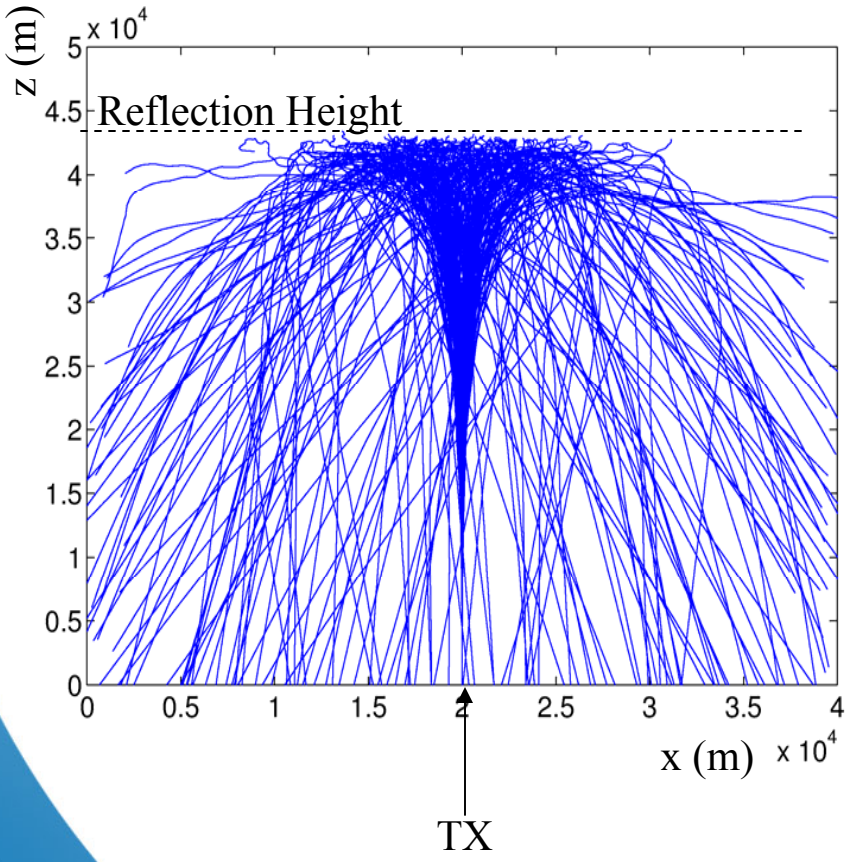

Angle Histogram

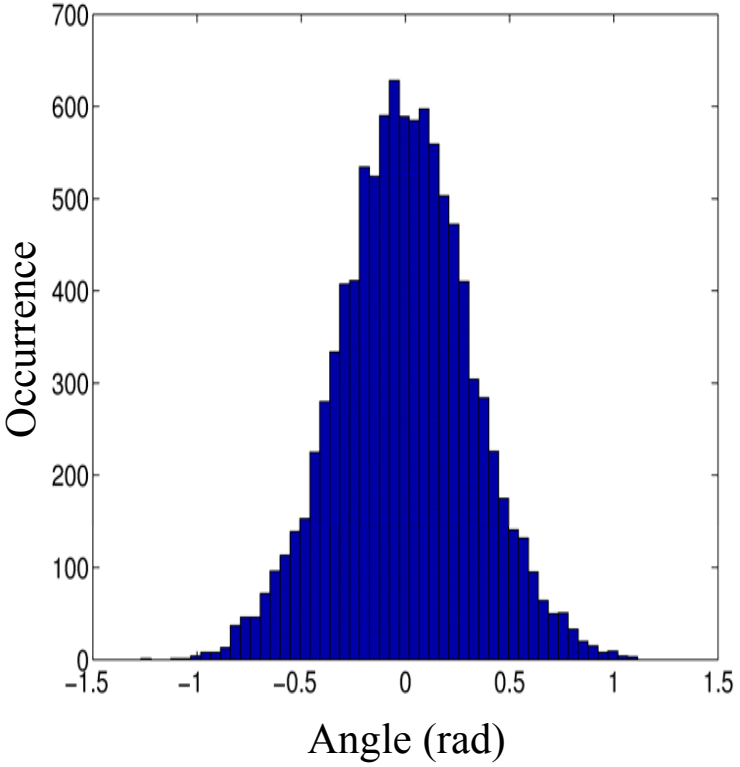

Measurements

- Measure "local wavenumbers" $K_x(x,y)$ and $K_y(x,y)$:

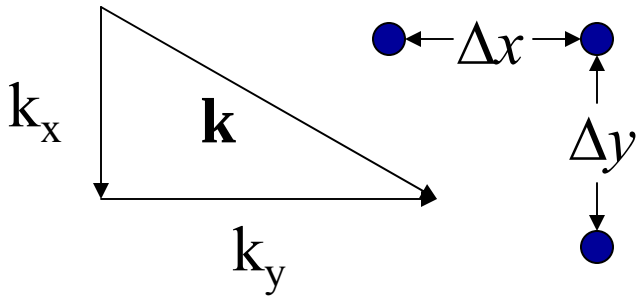

$$K_x(x,y) = \frac{\partial\theta(x,y)}{\partial x} \qquad K_y(x,y) = \frac{\partial\theta(x,y)}{\partial y}$$

- Φ is a field with random amplitude a and phase θ:

$$\Phi(x,y) = a(x,y)e^{i\theta(x,y)}$$

- Since $k_z^2 = (\omega/c)^2 - k_x^2 - k_y^2$ we need only $S(k_x,k_y)$:

$$S(k_x,k_y) = \iint E[\Phi^*(x,y)\Phi(x+X,y+Y)]e^{-ik_xX-ik_yY}\,dXdY$$

Measurements (con'd)

- Assume slowly varying condition, for all $m,n > 0$

$$\left|\frac{1}{a}\frac{\partial^m a}{\partial x^m}\right|, \left|\frac{1}{K_x}\frac{\partial^m K_x}{\partial x^m}\right| << \left|K_x^m\right| \qquad \left|\frac{1}{a}\frac{\partial^n a}{\partial y^n}\right|, \left|\frac{1}{K_y}\frac{\partial^n K_y}{\partial y^n}\right| << \left|K_y^n\right|$$

- a, K_x, K_y have joint PDF $f(a^2, K_x, K_y)$:

$$S(k_x, k_y) \approx (2\pi)^2 \int a^2(x,y) f(a^2, K_x, K_y) da^2$$

- Wavenumber PSD is power-weighted histogram of local wavenumbers
- Analogy: Frequency spectrum is spectrum of instantaneous frequencies if modulation rate << bandwidth

Measurements (con'd)

Skymap

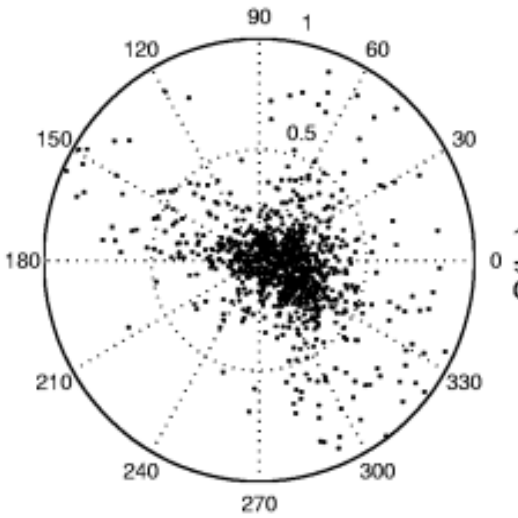

$S(k_x)$

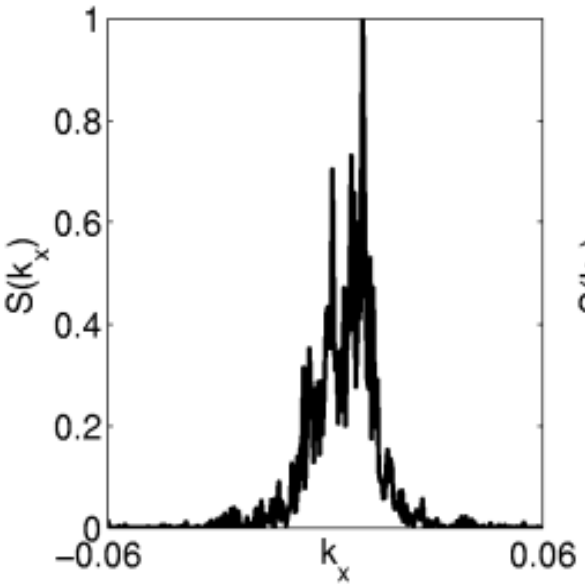

$S(k_y)$

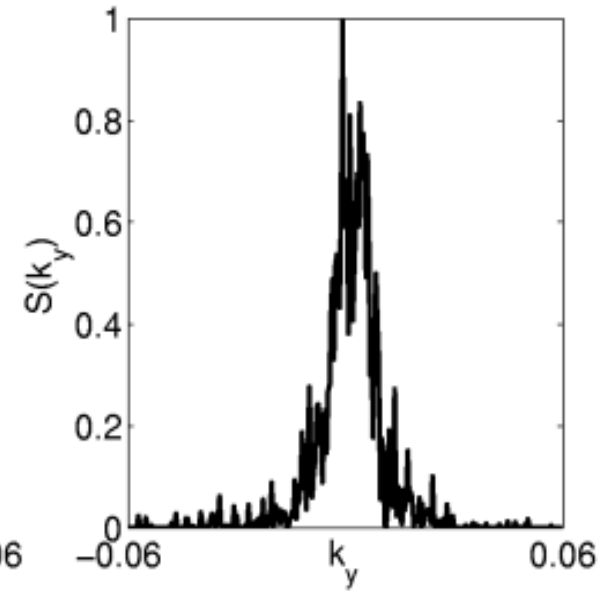

$$S(k_x, k_y) \approx \frac{2\pi}{\sigma^2} e^{-\frac{k_x^2 + k_y^2}{2\sigma^2}}$$

$$\text{spread} \approx 2\sigma / k$$

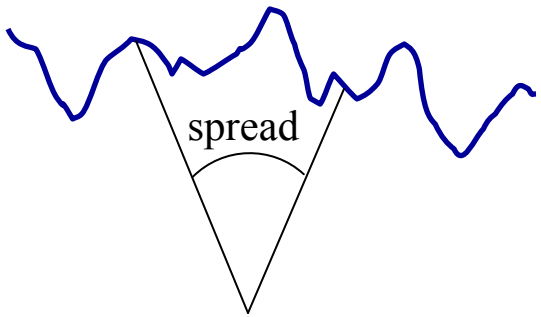

Analysis of Array Configurations

16 Linear

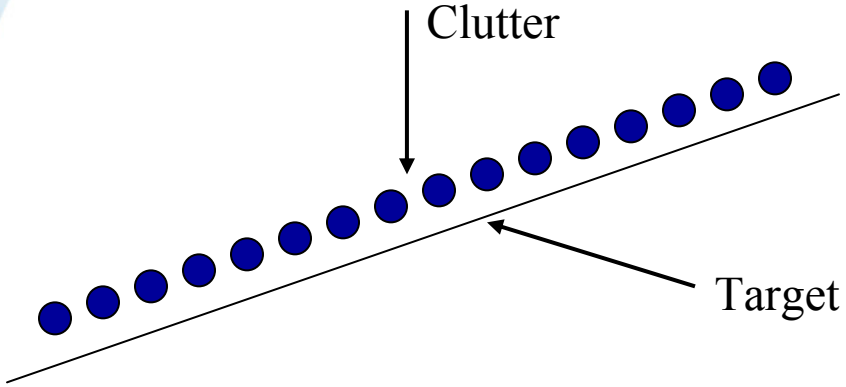

8x8 Cross

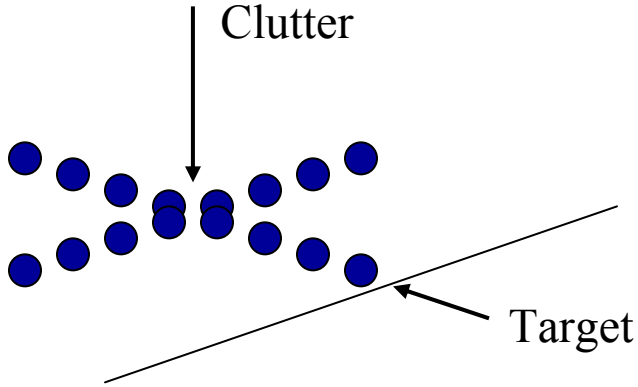

4x4 Filled Square

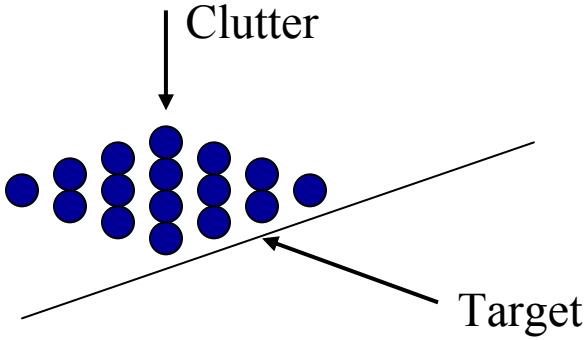

16 Circle

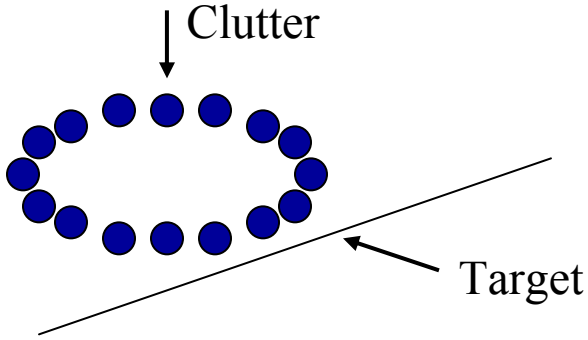

- From $S(k_x,k_y)$ calculate $\mathbf{R}_n$ and Array Gain A

Array Gain Versus Target Azimuth

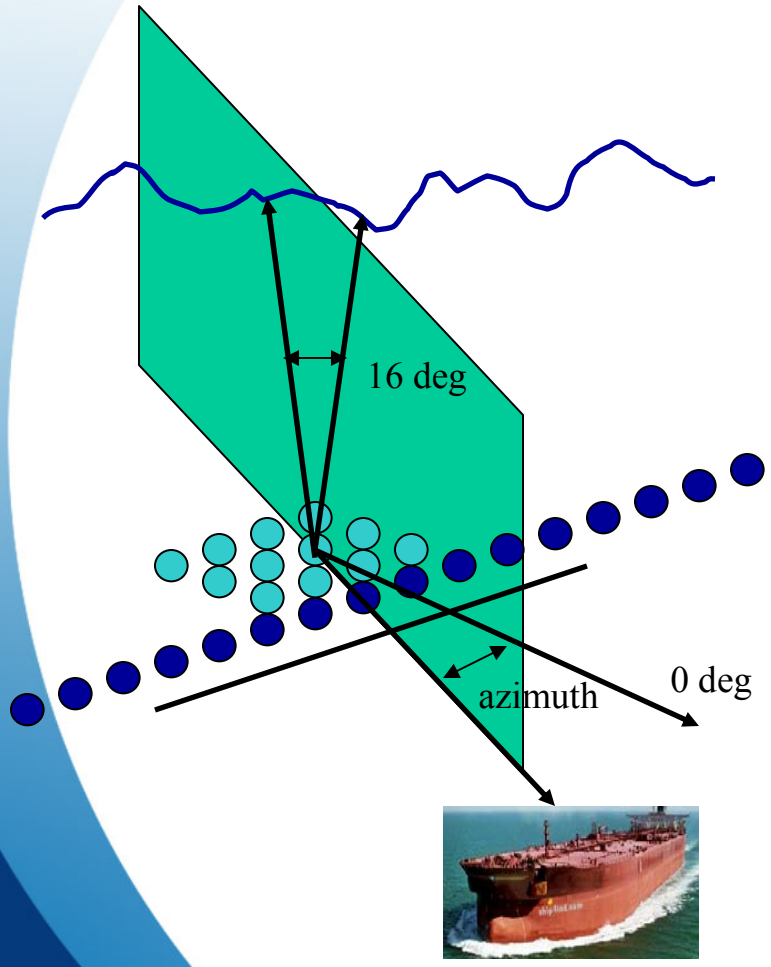

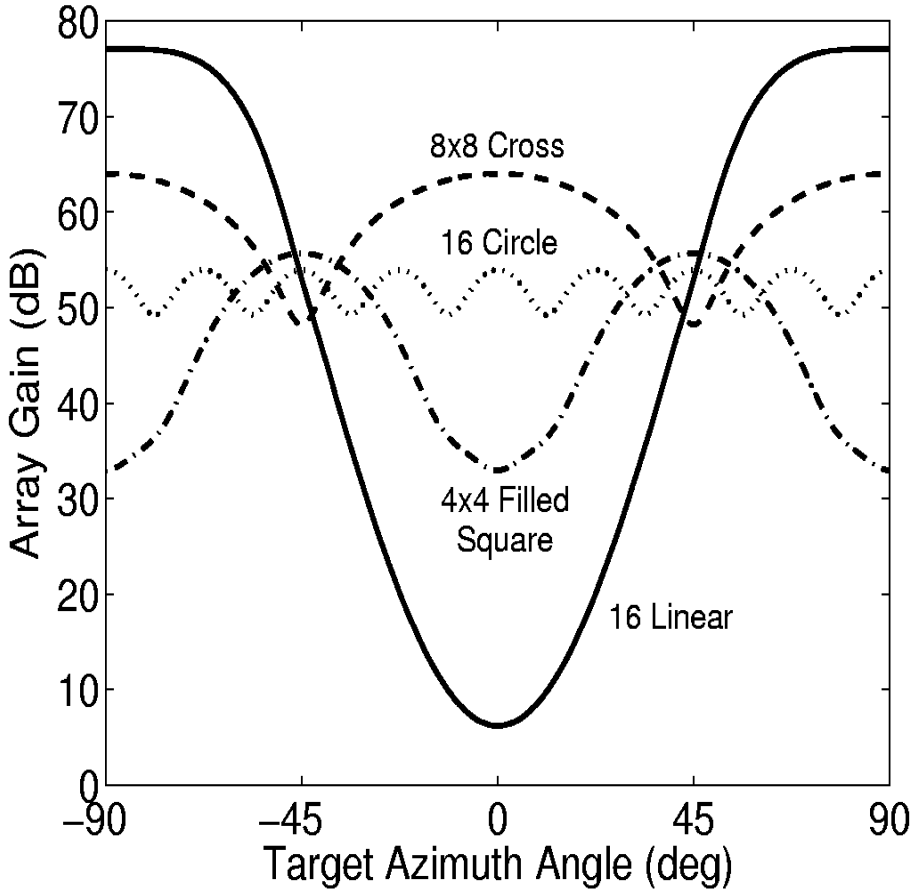

Array Gain Versus Clutter Spread Angle

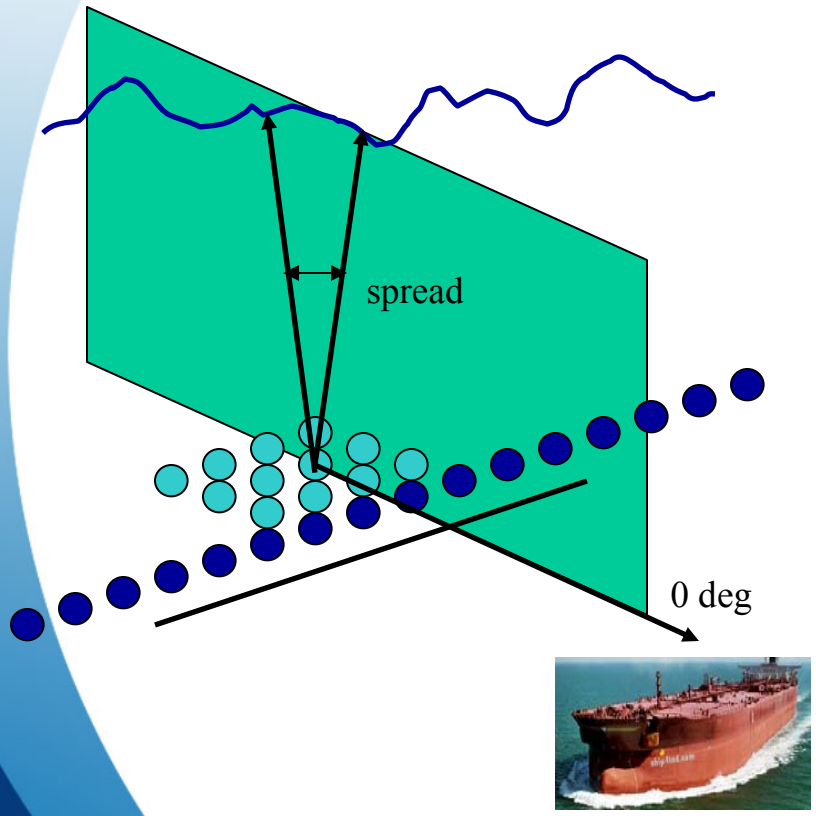

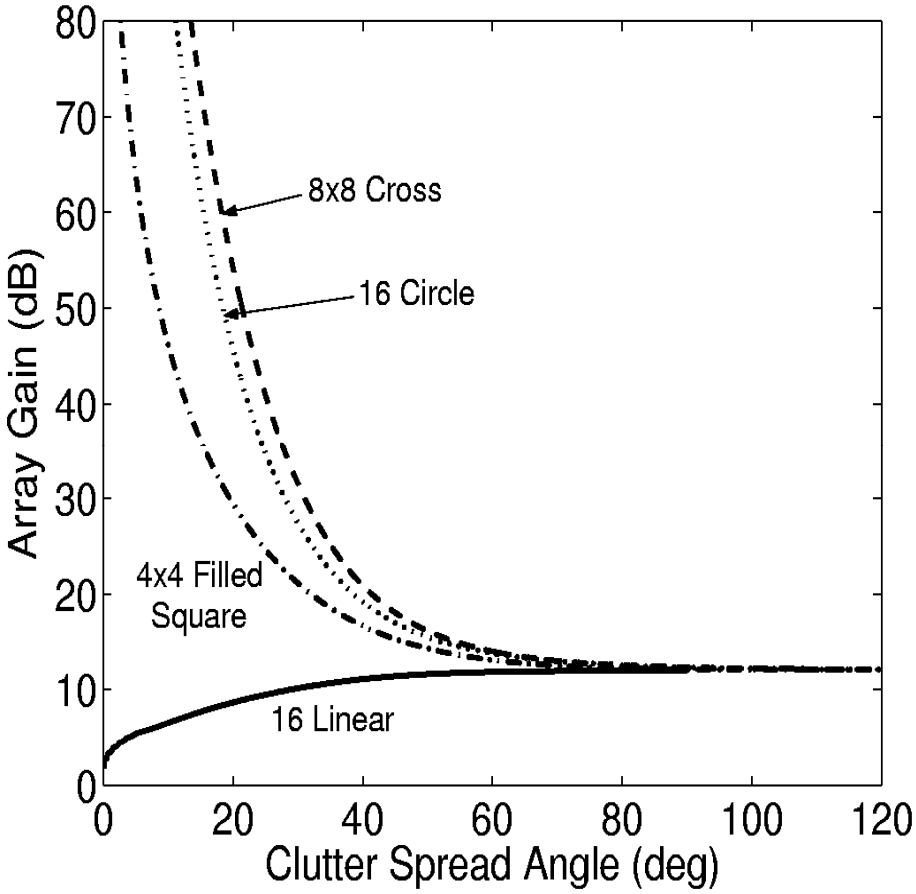

Linear Array: Broadside Versus Endfire

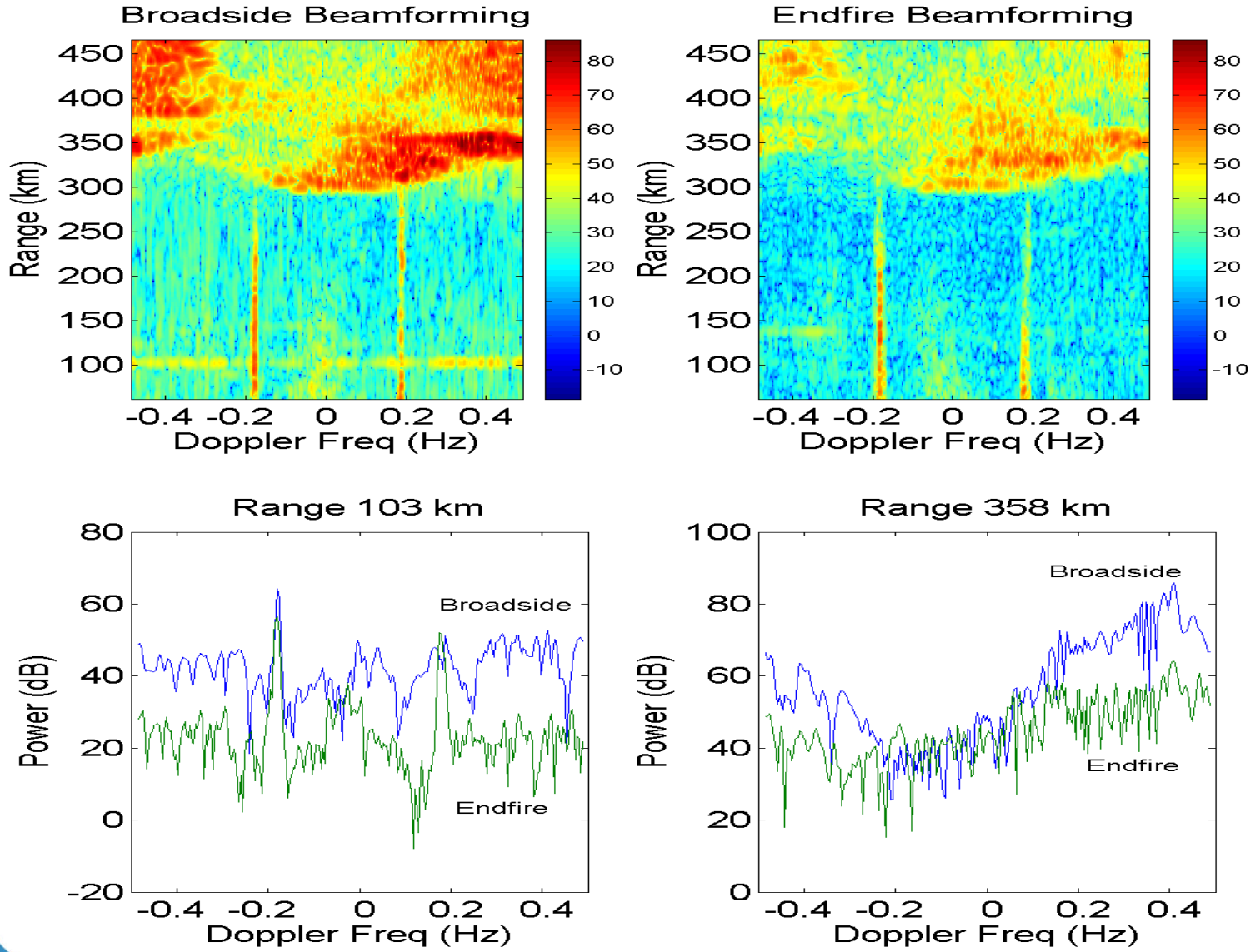

Problem of Mixed-Path Propagation

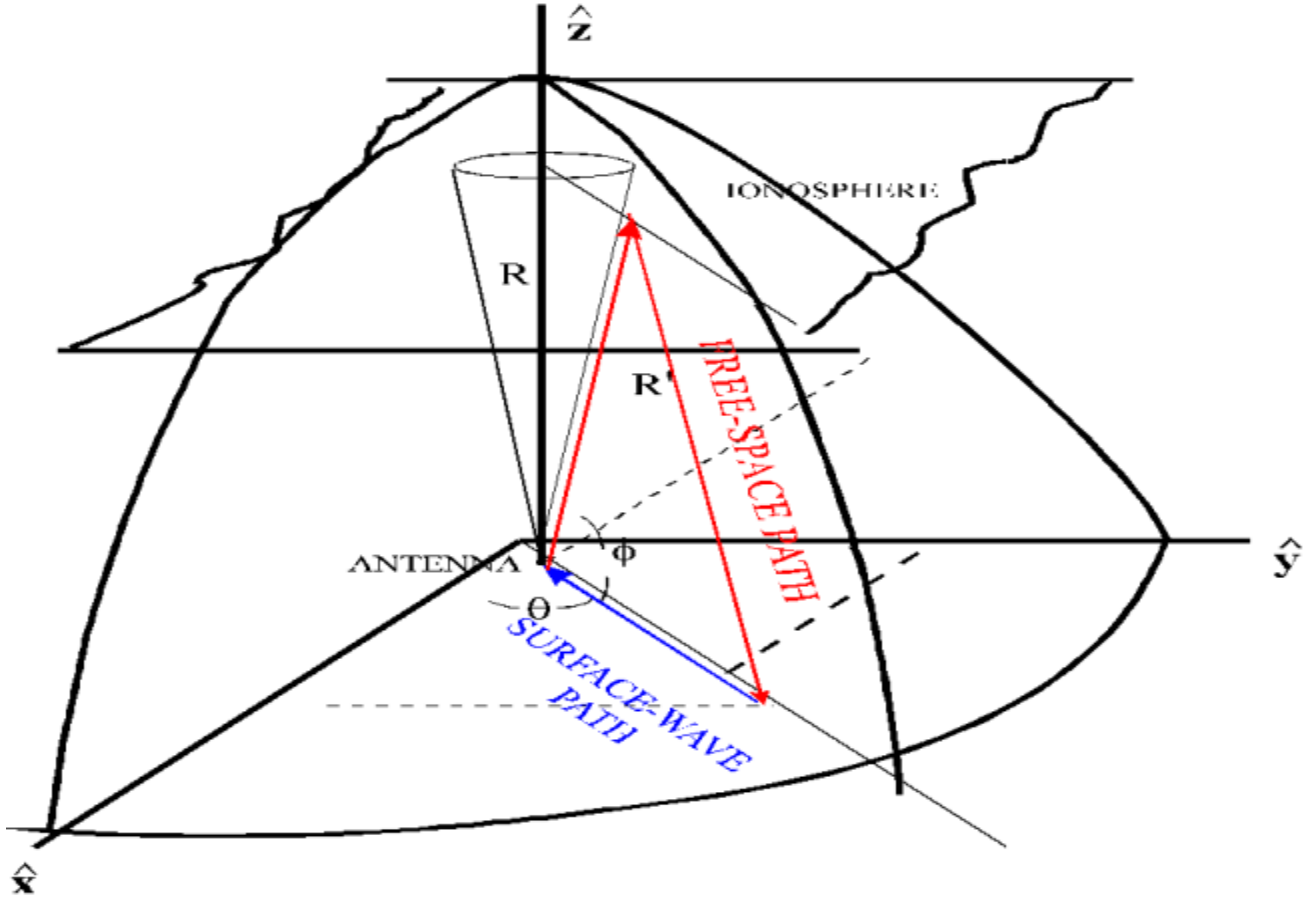

- Can exceed Bragg line power by 40 dB

Current Work

- 2-D Array Experiment

- Joint Doppler-Angle Processing (STAP)

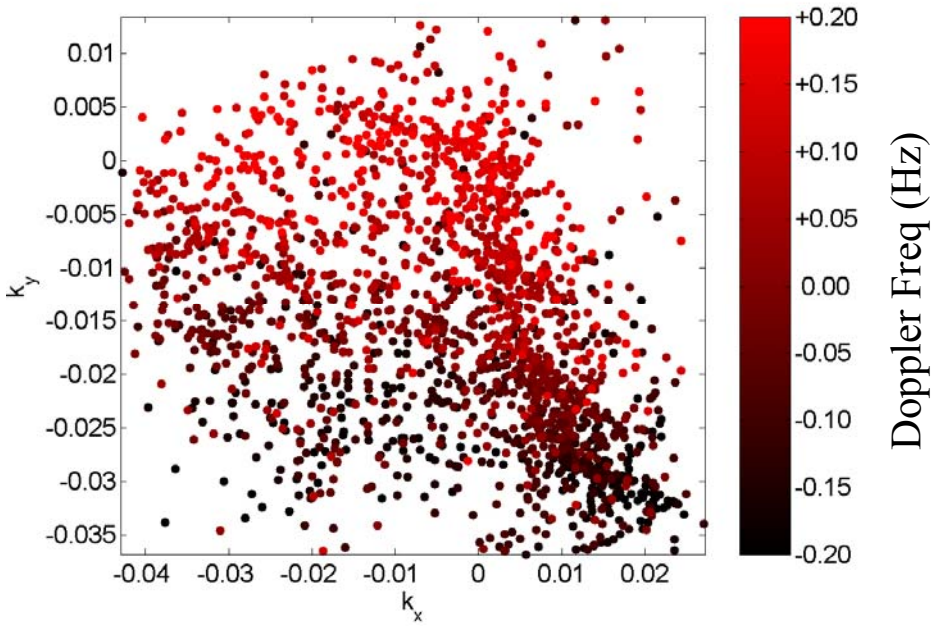

Conclusions

- Goal was to determine array gain *A* for various configurations
- Angular spectrum of clutter is Gaussian, spread ~15 deg
- Array gains vary with size of projection on vertical plane containing target azimuth
- Cross array produces best overall array gain for fixed number of sensors
- Performance constrained by mixed-path propagation or array calibration

The Defence Research and Development Agency

provides Science and Technology leadership

in the advancement and maintenance of

Canada's defence capabilities.